Catal Surv Asia (2008) 12:253–265
DOI 10.1007/s10563-008-9061-5

Layered Double Hydroxides as Catalytic Materials: Recent Development

Fazhi Zhang · Xu Xiang · Feng Li · Xue Duan

Published online: 15 November 2008
© Springer Science+Business Media, LLC 2008

Abstract This report surveys the recent development of layered double hydroxides (LDHs) as catalytic materials, which have attracted considerable attention in the past decade. A major challenge in the rapidly growing field is to improve the functionalities of these materials. Therefore, this article is mainly focused on the lately reported design and synthesis strategies for LDH materials and their catalytic applications as actual catalysts, catalyst precursors and catalyst supports.

Keywords Layered double hydroxide · Synthesis · Catalyst · Precursor · Support

1 Introduction

Layered double hydroxides (LDHs), also known as hydrotalcite (HT)-like materials, are a class of two-dimensional nanostructured anionic clays whose structure is based on brucite ($Mg(OH)_2$)-like layers. A fraction of the divalent cations coordinated octahedrally by hydroxyl groups in the layers are replaced isomorphously by trivalent cations, giving positively charged layers with charge-balancing anions in the hydrated interlayer regions. Some hydrogen bonded water molecules may occupy any remaining free space in the interlayer regions [1, 2]. The idealized layered structure of LDHs is shown in Fig. 1. LDHs may be represented by the general formula $[M^{II}_{1-x}M^{III}_{x}(OH)_2]^{x+}(A^{n-})_{x/n} \cdot yH_2O$, where M^{2+} (M = Mg, Fe, Co, Cu, Ni, or Zn) and M^{3+} (M = Al, Cr, Ga, Mn or Fe) are di- and trivalent cations, respectively, the value of x is equal to the molar ratio of $M^{2+}/(M^{2+} + M^{3+})$ and is generally in the range 0.2–0.33; A^{n-} is an anion. As a result, a large class of isostructural materials, which can be considered complementary to aluminosilicate clays, with versatile physical and chemical properties can be obtained by changing the nature of the metal cations, the molar ratios of M^{2+}/M^{3+}, as well as the types of interlayer anions.

LDHs, both as directly prepared or after thermal treatment, are promising materials for a large number of practical applications in catalysis, adsorption, pharmaceutics, photochemistry, electrochemistry and other areas. LDH materials have relatively weak interlayer bonding and as a consequence exhibit excellent expanding properties. Over the past few years, increasing interest has been devoted to the use of these layered inorganic solids as host materials in order to create host-guest hybrid (supramolecular) structures with desirable physical and chemical properties, in which the brucite-like layers may impose a restricted geometry on the interlayer guests leading to enhanced control of stereochemistry, reaction rates, and product distributions. The formation of three-dimensional pillared structures by appropriate intercalation process opens up new possibility for functional materials with novel properties.

In this article we review the development of synthesis methods for LDHs, and pay much emphasis on the recently reported LDH materials as actual catalysts, catalyst precursors and catalyst supports used in a variety of heterogeneous reactions.

F. Zhang · X. Xiang · F. Li (✉) · X. Duan
State Key Laboratory of Chemical Resource Engineering, Beijing University of Chemical Technology, P.O. Box 98, 100029 Beijing, People's Republic of China
e-mail: lifeng_70@163.com

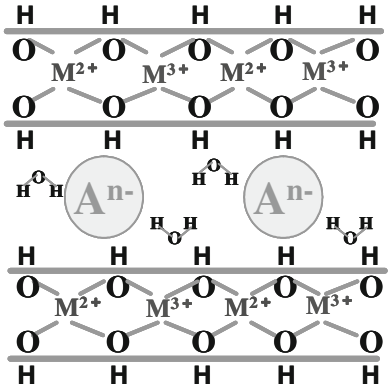

Fig. 1 The idealized layered structural illustration of LDHs

2 Development of Synthesis Methods for LDH Materials

Several reviews have comprehensively summarized various synthesis strategies and techniques of LDH materials during the past decade [3–5]. Herein, the article is mainly focused on the newly developed synthesis approaches of these materials, associated with the control on particle size, structure, morphology, crystallinity and orientation of the resulting LDHs. This greatly favors a further understanding and insight on the synthetic methodologies of the kind of materials.

It is well-known that the well-crystallized LDH crystals with large platelets in micrometer sizes could be obtained by urea or hexamethylenetetramine hydrolysis in homogeneous precipitation reactions [6–8]. However, the highly crystalline LDH materials were mainly restricted to Al^{3+}-containing LDHs, whereas the trivalent transition-metal LDHs such as Ni/Fe-LDH with high crystallinity and hexagonal shapes have not been obtained yet by homogeneous precipitation. Therefore, a new synthesis method of Ni/Fe-LDH has recently been developed using urea hydrolysis under the presence of trisodium citrate as chelating reagent [9]. The LDH material with high crystallinity and well-defined hexagonal shapes was produced under a hydrothermal condition of 150 °C and a period of 2 days. The chelating reagent played a functional role in the different reaction periods. Usually, amorphous $Fe(OH)_3$ is first precipitated during the reaction. Further urea hydrolysis leads to the conversion of $Fe(OH)_3$ to Ni/Fe-LDH. The addition of trisodium citrate makes the pH precipitation range of $Fe(OH)_3$ increase due to the chelating interaction of Fe^{3+} ions with trisodium citrate. Meanwhile, the added trisodium citrate in the form of $C_6H_5O_7^{3-}$ ion in the solution can induce Fe^{3+} ions to form the $[Fe(C_6H_5O_7)_2]^{5-}$ ligand instead of $Fe(OH)_3$. As a result, in the favorable concentration of Ni^{2+} and OH^- ions, Ni/Fe-LDH materials with high crystallinity and regular hexagonal shape can be produced.

Recently, a gas–liquid contacting route has been developed in our laboratory for the synthesis of Mg/Al- or Zn/Al-LDHs with interlayer CO_3^{2-} anions through the decomposition of ammonium carbonate [10]. The key feature was a pH gradient formed by the diffusion of NH_3 and CO_2 vapors in the metal salts solutions from solid $(NH_4)_2CO_3$ placed in a closed environment. The precipitation of LDHs occurred according to the following reactions (M was Mg or Zn):

$$(NH_4)_2CO_3 \rightarrow 2NH_3(g) + CO_2(g) + H_2O \quad (1)$$

$$NH_3 + H_2O \Leftrightarrow NH_4OH \Leftrightarrow NH_4^+ + OH^- \quad (2)$$

$$CO_2 + H_2O \Leftrightarrow H_2CO_3 \Leftrightarrow H^+ + HCO_3^- \Leftrightarrow 2H^+ + CO_3^{2-} \quad (3)$$

$$2OH^- + (x/2)CO_3^{2-} + (1-x)M^{2+} + xAl^{3+} + yH_2O \rightarrow [M_{1-x}Al_x(OH)_2](CO_3)_{x/2} \cdot yH_2O \quad (4)$$

The pH gradient had a key effect on the nucleation and growth of LDH particles. After nucleated in surface layer of salts solutions, LDHs gradually subsided to the bottom of vessels due to gravity effect. Because of the formation of pH gradient, the supersaturation faded away and the growth of LDHs terminated when LDHs subsided to a certain position. As a result, the LDHs subsided on the bottom of vessels had uniform crystalline size due to the termination of growth. The decomposition of $(NH_4)_2CO_3$ held the pH on surface layer steady, and the diffusion of NH_3 and CO_2 vapor led to the pH of solutions up to 10. At this stage, all LDH particles with uniform crystalline size came into aging. The results showed that these particles obtained by the method had well-crystallinity, uniform crystallite size. This method has been used to prepare LDHs with other cations such as Ni/Al and Ni/Fe with uniform crystallite size.

An innovative method of synthesizing LDH nanomaterials has been established in our laboratory instead of the conventional coprecipitation route [11]. The narrower particle size distributions for Mg/Al-LDH nanomaterials with different Mg^{2+}/Al^{3+} molar ratios could be prepared by a rapid mixing and nucleation in a colloid mill followed by a separate aging step, compared with conventional coprecipitation at constant pH. The colloid mill (see Fig. 2) consists of a conical rotor and a stator with a narrow gap (which can be varied in the range 2–10 μm) between them. A variable rotor speed in the range 3,000–5,000 rpm can be adjusted. The major advantages of the method were that it produced not only smaller crystallites with a higher aspect ratio, but also narrow distribution of crystallite size, compared to those from the coprecipitation process. In the colloid mill, the mixing and nucleation were completed in a very short time (around several minute) at room temperature followed by a separate aging or crystallization at

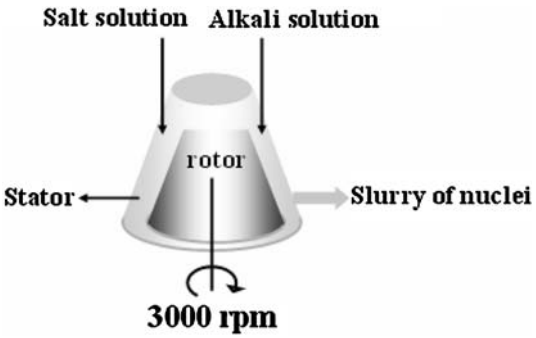

Fig. 2 Schematic illustration of a colloid mill

elevated temperature. In the highly turbulent zone of colloid mill, agglomeration of the nuclei was inhibited and the nuclei remained a tiny size due to high-speed rotation and shearing force. The resulting mixtures of nuclei with a narrow size range were aged in a separate stage, resulting in crystallites with a similarly narrow range of diameters.

In addition, Xu and co-workers developed a modified coprecipitation method for stable homogeneous LDH suspensions with controllable particle sizes [12]. This new method involved a fast coprecipitation of mixed salt solutions and alkali solutions at room temperature and ambient pressure followed by hydrothermal post-treatment under controlled temperature and time. The resulting LDH particle size can be controlled in the range of 50–300 nm with the aspect ratio about 5–10 by adjusting the synthetic conditions. A variety of cations, such as Ni^{2+}, Fe^{2+}, Fe^{3+}, and Gd^{3+} can be incorporated into the hydroxide layers and many anions, such as Cl^{-}, CO_3^{2-}, and NO_3^{-}, can be intercalated into the interlayer galleries, as well as DNA and drug molecules. The positively charged LDH platelets escaped from the aggregates through Brownian motion and were suspended as stable colloids. An important prerequisite for complete segregation of LDH platelets was to remove extra salts prior to hydrothermal treatment. Hydrothermal treatment resulted in a more even distribution of cations in layers, a more regular crystallite shape, and growth of individual crystallites via cation diffusion and crystallite repining.

Besides particle sizes and size distributions, the LDH morphologies are also an interest issue for controlled growth. A wide range of studies has been carried out either on the chemical/physical nature or on the application of reverse micelles/microemulsions to produce well-defined inorganic structures. In space-confined reactions, reverse micelles/microemulsions are used to disperse reactants and act as microreactors providing limited space for the reactions. Inorganic nanocrystals with uniform size distributions are thus prepared. A novel water-in-oil reverse microemulsion system has been applied for the first time in the synthesis of Mg/Al-LDHs with unique morphologies [13]. The used system is the reverse microemulsion of sodium dodecyl sulfate-water-isooctane with water/surfactant molar ratio of 24. The nanometer sized LDH platelets typically with a diameter of 40–50 nm and thickness of 10 nm were obtained. LDH structures of different growth orientations can be induced by a further modified reverse microemulsion using triblock copolymers as soft-template during crystallization. The results showed that the aspect ratio of LDHs can flexibly be adjusted over a wide range, which may result in unique chemical or physical properties for extended applications. Also, hydrophobic LDH monolayers could be synthesized in a reverse microemulsion system by one-step route [14].

Inorganic hollow spheres with well-defined chamber architecture were of particular interest because of their high surface area, low density and good permeability. A general approach was to use a sacrificial template, on which shell materials were deposited in a controlled manner e.g., a self-assembly technique. Hollow nanoshells of LDHs have been fabricated using exfoliated LDH nanosheets as a shell and building block and polystyrene (PS) beads as a sacrificial template [15]. The whole synthetic route mainly involved three steps, firstly layer-by-layer assembly of delaminated LDH nanosheets onto the PS surface and poly(sodium 4-styrene sulfonate) (PSS), secondly thermal decomposition to remove the PS core and PSS, and finally reconstruction of LDH structure in humid air by employing the memory effect of LDHs. The unique hollow structure of LDH will be useful in bio- or environmental applications such as drug storage and release, enzyme immobilization and pollutant adsorption.

The macroporous materials with three-dimensional periodicals are currently interesting for a wide range of applications considering their porosity, such as in catalysis, filtration, molecular sieving, and chemical/bio sensors. A typical strategy to prepare three-dimensional ordered macroporous structures is to employ colloidal crystal (opal) as a sacrificial template. So-called "inverse opals" are formed by infiltrating the interstitial voids of the opal with the desired precursor solution forming macroporous inorganic structures after fluid–solid transformation and subsequent removal of the opal arrays. Leroux et al. has reported on a general method to prepare three-dimensional ordered macroporous (3-DOM) LDH replicas by coprecipitation of divalent and trivalent metal cations in the interstices of PS colloidal crystals and successive infiltrations, and subsequent removal of PS template through dissolved in organic solvent (e.g., toluene) [16, 17]. The Mg/Al-LDH with CO_3^{2-} anions was firstly prepared by this method [16]. Subsequently, this method was extended to produce various 3-DOM LDH materials with tunable layer compositions and intercalated guest anions. The relevance of structure and catalytic property was also

investigated [17]. The photocatalytic tests showed that decatungstate intercalated 3-DOM LDHs displayed a higher activity in the photodegradation of 2,6-dimethylphenol than the decatungstate intercalated LDHs prepared by a conventional coprecipitation method. Therefore, the structure of 3-DOM LDH materials could enhance the LDH performance in many potential applications.

Organizing LDH microcrystals into uniformly aligned 2D arrays or large films, particularly oriented LDH films, might lead to innovative properties and enhanced performance of LDH materials in such conventional fields. Pinnavaia et al. fabricated transparent and smooth films consisting of the oriented LDH microcrystals by colloidal suspensions of LDHs from hydrolysis of LDH/methoxide [18]. Jung and co-workers obtained a monolayer assembled LDH films with high packing density and preferred c-axis orientation perpendicular to the substrate surface by a facile ultrasonification of LDH nanocrystals [19–21]. Our group reported the fabrication of Mg/Al-LDH films using an external aluminum source under hydrothermal conditions on sulfonated polystyrene substrate [22]. The microstructure of LDH films could be controlled by adjusting the preparation conditions, e.g., the sulfonation degree of the substrate, the total concentration of metal cations in the solution, and the reaction temperature [23]. The kinetics mechanism of the film formation agreed with a second-order exponential nucleation law, suggesting that the film formation involved first transportation of metal cations to the surface of the substrate, adsorption, and then enrichment of the cations followed by nucleation and eventually oriented growth of films at the phase boundary.

Growing thin films directly from a substrate will be greatly favorable to the adhesive property and the mechanical stability of the film, compared to colloidal-deposition techniques. Therefore, we developed an in situ growth method to prepare oriented Ni/Al-LDH films with curved hexagonal structures by using porous anodic alumina/aluminum (PAO/Al) as both substrate and sole aluminum source [24]. The surface microstructure of the LDH film can be tailored by adjusting the crystallization temperature and time. The organically modified LDH films showed excellent superhydrophobicity with high water contact angle of above 160°, which was attributed to the nest-like microstructures on the surface of the films.

In the recent study, we found that a suspension of monodisperse LDH nanoparticles could be used for fabrication of large transparent self-supporting films of LDHs by a simple solvent-evaporation technique [25]. Suspensions of Zn/Al- and Ni/Al-LDH nanoparticles were prepared in the colloid mill [6]. The interlayer nitrate may be ion-exchanged by a variety of inorganic or organic anions, for example rare-earth ethylenediamine tetraacetic (EDTA) complex. The resulting LDH suspensions after dilution were contained in a vessel and dried in air. Transparent self-supporting films with dimensions up to centimeters can be peeled off from the internal surface of the vessel. The thickness of film can be controlled by adjusting the concentration of the suspensions and the drying conditions. The self-supporting films had the characteristics of sufficient thickness, mechanical robust and a high degree of optical transparency. The oriented films allowed detailed study of host–guest interactions in LDHs and delicate measurement of anisotropy of functional guest anions in the interlayer of LDHs.

3 Catalytic Applications of LDH Materials

The properties of LDHs and derivative materials can be tailored by altering the types of cations in the layers, the molar ratios of cations, the nature of the compensating anions in the interlayer space, and the synthesis and dehydration/rehydration conditions [26]. Therefore, LDHs have been greatly concerned with their great applications as actual catalysts, catalyst precursors and catalyst supports [27].

3.1 Actual Catalysis

Solid catalysts are currently receiving considerable attention from the viewpoint of environmental and economical concerns because of their unique properties such as simple handling, easy separation and recyclability, and low cost [28]. In the search for environmentally benign and recyclable catalysts for replacing homogeneous catalysts, activated LDH materials, due to their unique ability to give Brønsted type base sites, are of current interest as solid base catalysts in several important organic reactions, such as Knoevenagel condensations, Michael additions, Claisen–Schmidt and aldol condensations. Further, calcined LDHs with rock-salt-like structures, possess acid and basic sites. The nature, strength and relative amounts of these sites depend essentially on the nature and molar ratio of cations, and the calcination temperature.

The features emphasize that LDHs are very attractive for these types of reactions due to their ability to give acid–base bifunctional catalysts. Generally, the approach applied for activation of LDHs firstly involves a thermal treatment, leading to the dehydration of LDHs and the sequential destruction of the layered structure to some extent. The next step is reconstruction of the layered structure by rehydration of LDHs in an appropriate medium (e.g., in an aqueous solution or moisture). The reversible dehydration–rehydration behaviors of LDHs depend on the "memory effect" i.e., the hydroxyl or water molecules can re-enter into the interlayers of dehydrated LDHs or calcined LDHs

because of the flexible intercalation capability in the interlayer space, resulting in the recovery of the layered structure. After rehydration, Brønsted base sites (OH^-) are thus incorporated into the interlayer [29]. Although the research devotion, the catalytic performance of reconstructed LDHs as a function of the rehydration is not well understood. The rehydration of the LDHs crystallites is a dominant factor controlling the number and the strength of OH^- active sites in solid base catalytic reactions. Medina and co-workers investigated the structure-activity relationships of activated Mg/Al-LDHs in different reconstruction manner and emphasized on the active nature of Brønsted basic sites for various aldol condensation reactions [30]. Liquid or gas phase rehydration procedures have been applied to reconstruct calcined LDHs. A superior catalytic performance has been found in the aldol condensation of citral with ketones and in the self-aldolization of acetone for the Mg–Al mixed oxide rehydrated in the liquid phase, compared to that rehydrated in the gas phase. The difference in surface areas, the number of basic sites and their accessibility for the two samples were the main factors for enhancing the catalytic activity. The number of OH^- groups and their nature were very similar in two samples, and only a small fraction of the basic sites in the rehydrated samples was active in aldol condensations. These results supported the proposal that only basic sites near the edges of the LDH platelets were active in aldol reactions. This work provided us a way to enhance the catalytic activity of LDHs by adjusting their rehydration procedure.

Roeffaers et al. adapted real time monitoring of the chemical transformation of individual organic molecules by fluorescence microscopy to monitor reactions catalyzed by a crystal of an LDH with the formula $[LiAl_2(OH)_6](OH) \cdot nH_2O$ [31]. They found the activity of base catalysis by LDH is not always associated with the same type of hydroxyl groups and that *trans*-esterification occurs mainly at the {0001} plane. When OH^- anions were introduced into the interlayer via calcination/rehydration, the CO_3^{2-} and other anions on the surface were also replaced by OH^-. Furthermore, they found that the hydroxyl groups were arranged in an ordered manner on the LDH surface. Ebitani et al. also found that the LDH surface can act as a macro-ligand providing an ordered array of OH^- and O^- groups which facilitates the assembly of trimeric $Ru^{IV}Mn^{IV}Mn^{IV}$ units in situ on the surfaces [32].

Recently, our group prepared the activated Mg/Al-LDHs with hydroxyl anions via calcination/rehydration of Mg/Al-LDHs synthesized by the urea decomposition method (U-RLDH) and the conventional titration co-precipitation method (T-RLDH), respectively [33]. Compared with T-RLDH, U-RLDH has highly crystalline, much larger particle size and regular platelet morphology. High-resolution transmission electron microscopy confirmed that the U-RLDH retains the lattice structure of the LDH precursors with lattice parameters $a = 0.31 \pm 0.01$ nm. The results indicated that they are both acidic and basic hydroxyl groups on the surface of LDHs, which can form acid–base pairs with a separation of 0.31 nm. An acid–base catalytic mechanism has been proposed to interpret the catalytic behavior based on the fact that acid–base hydroxyl group pairs on the activated LDH surface have a separation of 0.31 nm. The U-RLDH displayed higher catalytic activity in aldol condensation of acetone to afford diacetone alcohol (DA) than T-RLDH sample. The result is presented in Table 1. Consequently, it is concluded that the active sites are mainly located on the ordered array of hydroxyl sites on the vassal surface rather than on the defect sites. Previous studies suggested that the activity of activated LDHs in aldol reactions had a correlation with the surface area (in the range 200–400 m^2/g) [34]. Other reports had indicated that the activity increases with decreasing lateral size of the LDH particles, i.e., the particles with smaller size result in higher catalytic activity [35]. However, in this work, the U-RLDH having a large lateral size ($\sim$4,000 nm) and relatively low surface area ($\sim$140 m^2/g) showed a much higher activity than T-RLDH, despite the smaller lateral size and higher surface area in the latter. This suggested that the activity of activated LDHs is not mainly related to the surface area of the exposed edges. The findings suggested the regular lattice positions in the layers of LDHs, rather than the defect sites, act as catalytic active sites. This may stimulate the development of new type of catalysts. Furthermore, the Mg/Al-LDHs films were also fabricated in situ onto anodic aluminum oxide (AAO)/aluminum substrate [36]. The rehydrated LDH (RLDH) platelets, activated by calcination/rehydration, remained to be firmly immobilized on the AAO/aluminum and retained the hexagonal morphology similar to that of LDH parents. The catalytic performance for the aldol condensation of acetone

Table 1 Physico-chemical Property and Catalytic Data of Activated LDH Samples

Catalysts	T-RLDH	U-RLDH
Crystallite size in *a* direction/nm	180	3,900
Crystallite size in *c* direction/nm	66.4	84.9
Specific surface area/m^2g^{-1}	185	184
Acetone conversion to DA after 60 min/%[a]	3.0	8.3
Acetone conversion to DA after 180 min/%[a]	10.2	15.8
Acetone conversion to DA after 300 min/%[a]	14.4	19.6
Time to reach equilibrium/min	1,730	560

[a] The conversion of acetone to DA over different catalysts at 273 K with acetone/catalyst = 2 mol/0.3 g

showed that the RLDH film was superior to its counterpart in powder form.

In addition, Zhang et al. synthesized a nano-scale magnetic solid base catalyst Mg/Al-LDH/$MgFe_2O_4$ by calcination/rehydration and evaluated the catalyst using self-condensation of acetone as a probe reaction [37]. It was found that the Brønsted base catalytic layers of Mg/Al-LDHs were coated over magnetic $MgFe_2O_4$ cores through Mg–O–Fe and Al–O–Fe linkage, and the catalytically active OH^- sites in the interlayers were also exposed on the particle surface. This structure led to high activity, and the conversion to DA reached the thermodynamic equilibrium value of 23% at 273 K. The magnetic nano-scale solid base catalyst enabled simple and effective reclamation of the catalyst at the end of the reaction by using an external magnetic field. When the reclaimed catalysts were used in the next run, their activities remained still.

Activated Mg/Al-LDHs could exhibit high catalytic activity and selectivity in aldol condensation reactions at low temperatures upon loaded onto a kind of support material. For example, activated Mg/Al-LDHs with a lateral size of 20 nm deposited on carbon nanofibers (CNFs) showed a specific activity four times than that of unsupported LDHs in acetone condensation reaction [38]. Due to the small crystallite size of LDHs and the accessible pore of the CNFs support, a large number of accessible OH^- can be produced. This led to the improvement of catalytic activity.

In^{3+}-containing LDHs (Mg/Al/In-LDH and Mg/In-LDH) with the $Mg^{2+}/(Al^{3+} + In^{3+})$ molar ratio of 3.0 have been prepared by Li et al. [39]. The basic properties of the as-synthesized LDHs and calcined LDHs at 500 °C were investigated by the adsorption isotherms for phenol from cyclohexane solution. The results showed that the overall numbers of basic sites of calcined LDHs are higher than those of LDHs, and the calcined LDHs exhibited higher catalytic activity for Knoevenagel condensation of ethyl cyanoacetate with benzaldehyde than as-synthesized LDH sample. This is because of the fact that the different base site types are present in LDHs with carbonate anions and their calcined derivatives: the weak basic sites in LDHs come from OH^- groups on the lattice, whereas the strong basic sites in calcined products are associated with surface OH^- groups as well as O^{2-} centers linked to metal atoms. Furthermore, it is interestingly noted that the conversion of ethyl cyanoacetate increased with the density of base sites on the surface of materials.

The effects of structure and morphology of catalysts on the catalytic behavior were lately investigated in our group besides the composition of catalysts [40]. MgAl-LDHs were firstly grown in situ in the channels of the γ-Al_2O_3 macrospheres by urea hydrolysis. The magnesia-rich magnesium aluminate spinel (MgO–$MgAl_2O_4$) was prepared by calcination of LDHs and selective etching of excess aluminum with alkali solution. The resulting MgO–$MgAl_2O_4$ has a spherical framework structure composed of nanosized rod-like particles. The material exhibited a higher biodiesel yield in methanolysis of soybean oil than MgO/$MgAl_2O_4$/γ-Al_2O_3 with the same loading of magnesium prepared by an impregnation/calcination method. The enhanced catalytic activity of MgO–$MgAl_2O_4$ catalyst could be ascribed to its higher basicity, resulting from high specific surface area and large pore volume.

On the other hand, base species-intercalated LDHs can be used as efficient and environmental solid base catalysts in various organic transformations [41–44]. For example, F^--intercalated Mg/Al-LDH catalysts, which were prepared through an ion exchange of OH^- obtained in situ by calcination (450 °C) followed by rehydration of the LDH, displayed unprecedented catalytic activity both in Knoevenagel and 1,4-Michael reactions under mild liquid phase conditions at a greater rate compared with known solid bases and fluoride catalysts [42]. Also, *t*-butoxide ($^tBuO^-$) -intercalated Mg/Al-LDHs were found to be an efficient solid base for highly selective Wadsworth–Emmons (WE) reactions for the simple synthesis of α,β-unsaturated esters and nitriles [43]. Here, the $^tBuO^-$ anion is the sole contributory factor for activity in the WE reaction. More recently, diisopropyl amide ion was introduced into the interlayer of LDHs by ion-exchange with LDHs containing interlayer nitrate anion. The ion-exchanged sample and its calcined product were efficient and selective solid bases for aldol, Knoevenagel, Henry, Michael, *trans*-esterification and epoxidation reactions under liquid phase conditions [44].

3.2 Catalyst Precursors

3.2.1 Precursors of Metal Oxide- or Metal-Supported Catalysts

LDHs can be suitable precursors for metal oxide- or metal-based heterogeneous catalysts. Upon calcination and/or sequent reduction, these materials usually give rise to well-dispersed and supported metal oxides or metal particles over mixed oxide matrix, providing active sites in the catalytic reactions (Fig. 3).

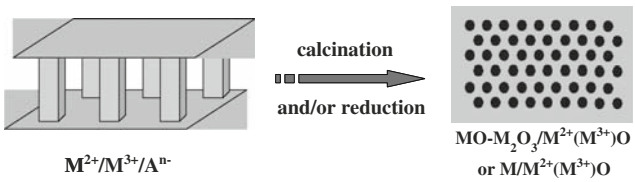

Fig. 3 Simplified representation of the calcination and/or reduction process of LDHs

Many groups have reported the use of calcined LDHs as heterogeneous catalysts in the liquid-phase catalytic reactions. For example, Ni/Al-, Ni/Al(Sn)-, Co/Al- and Co/Al(Sn)-LDHs were tested in decomposition of methanol, partial oxidation of methanol (POM), steam forming of methanol (SRM), and oxidative steam reforming of methanol (OSRM) reactions, for the purpose of H_2 production for fuel cells [45]. Zhang et al. have prepared a series of Cu-based LDHs [46, 47], and found that the calcined LDHs with Cu/Zn/Al molar ratio of 1:1:1 has the highest catalytic activity for the oxidation of aqueous phenol solutions by hydrogen peroxide at room temperature and atmospheric pressure, and that the oxidation products indicated the presence of phloroglucinol, hydroquinone and catechol, as well as deep oxidation organic products such as acetic acid and acetone. According to the structural characteristics, it can be concluded that the calcined Cu/Zn/Al-LDH catalyst may be related to the formation of a great amount of composite metal oxide containing Cu^{2+} and high dispersion of active copper centers present on the surface.

Increasing uses of fossil fuels such as coal, natural gas and petroleum for power generation and transportation have greatly increased NO_x emissions in the past decade, inevitably leading to a series of serious environmental problems even disasters. Thus, the elimination of NO_x is becoming a more and more urgent mission to chemists and related researchers. The catalysts that can effectively reduce NO_x in the presence of excess O_2 are now widely sought. The NO_x storage/reduction (NSR) catalyst [48, 49], which are used in engines that alternately operate under lean-burn and rich-burn conditions [50, 51], may be a good candidate. Lately, a kind of well-dispersed mixed-oxides derived from LDHs has attracted considerable interest in the search for alternative NSR catalysts [52–54]. Recently, Xu et al. designed and developed multi-functional, mixed $Ca_xCo_{3-x}Al$-oxide catalysts that elegantly combined the catalytic capability of transition metals for NO_x decomposition, storage, and reduction on the basis of LDH compounds [55, 56]. The excellent performance of catalysts possibly benefited from the good dispersion and the elegant combination of active components. The work here strongly indicated that the transition-metal mixed-oxide catalysts for effective NO_x transformation could be rationally synthesized by the combination of transition metals in the LDHs precursor and would be important and excellent catalysts in environmental application.

Our recent studies have suggested that Co- or Ni-containing LDHs are good catalyst precursors for the growth of carbon nanomaterials. Cobalt nanoparticles were produced by calcination and subsequent reduction of Co/Al-LDH precursors [57]. Multi-walled carbon nanotubes (CNTs) with uniform diameters were grown on the catalytically active Co particles with a diameter of around 15 nm by catalytic chemical vapor deposition (CCVD) of C_2H_2, due to the high dispersion of metal particles and large surface area of resultant mixed oxides. The specific surface areas of calcined Co/Al-LDH and the CNTs after purification reached 131 and 215 m^2/g, respectively. The precursor route for a Co-based catalyst enables scalable preparation of CNTs at low cost. More lately, the supported Co/Al-LDH has been used as precursor for growth of novel carbon nanostructures [58]. Three types of carbon nanostructures (tubes, caterpillar-like fibers and interwoven spheres) were grown onto silicon-supported catalyst from a Co/Al-LDH precursor. The morphologies of carbon nanostructures can be tuned by simply adjusting the growth duration. The growth mechanism was proposed on the basis of an overgrowth of the initially formed tubular nanostructures. Interestingly, the as-grown caterpillar-like fibers and interwoven spheres exhibited water contact angle as high as $163 \pm 2°$ and $168 \pm 2°$, respectively, exhibiting excellent surface super-hydrophobicity. This may originate from the presence of the unique surface networks. The super-hydrophobic property can extend the application of these carbon nanostructures in surface engineering, e.g., antiwetting coatings or micro-liquid transfers.

In addition, a novel Ni/Al-LDH/carbon (LDH/C) hybrid composite has also been used as catalyst precursor for the catalytic growth of CNTs [59]. The LDH/C composite with interwoven structure was prepared by the crystallization of Ni/Al-LDH simultaneously accompanied by the carbonization of glucose under mild hydrothermal conditions. After the controlled thermal conversion, high-surface-area nickel-based mixed-metal oxides with interconnected mesopore network were generated due to the removal of carbon. The specific surface area of calcined LDH/C composite at 450 °C can be as high as 288 $m^2\ g^{-1}$, associated with small pore size and mesopore network. The catalytic studies suggested that the Ni-based mixed oxides have superior catalytic activities for the growth of CNTs. The grown CNTs had uniform diameters and less structural disorder, compared to their counterpart grown on the catalyst derived from LDH precursor. This can be attributable to high dispersion and small size of Ni nanoparticles on the high-surface-area mixed oxides after reduction. Such a tunable mesopore network of Ni-based mixed oxides should be desirable in more extensive fields related to heterogeneous catalysis.

Conversion of natural gas into more valuable products by reforming reactions is of major importance for effective use of energy source. High-performance catalysts for reforming reactions are required with a high activity and selectivity for the target products, CO and H_2, and with a low selectivity for coke formation. During the past two decades, it is agreed that Ni/Mg(Al)O catalyst based on LDH precursor is a

active catalyst for wet or dry reforming of methane, most likely due to an optimum combination of basicity of the support, metal particle size, and/or an electronic "spillover" effect of the carrier material [60, 61]. Olafsen et al. in a recent report exploited the fourth possibility [62] that is, a direct participation of the LDH carrier material in the reactions. They found that in the dry reforming of propane to synthesis gas, CO_2 was adsorbed on the basic Mg(Al)O carrier and acted as a permanent source of oxygen for the metallic Ni, and thus propane could react rapidly with Ni–O species to produce CO and H_2O.

Not only the transition metals in the layers of LDHs can give rise to the supported metal particles after calcination and reduction, but also transition metal complex intercalated LDHs can lead to a high degree of dispersion of metal particles on the mixed oxides subjected to similar post-treatment. Intercalation of nickel hydroxy citrate colloids of controlled charge and size in the interlayer galleries of Mg/Al-LDH by anion exchange resulted in the formation of Ni colloid-Mg/Al-LDH nanocomposites [63]. The fine control in size and distribution of the reduced Ni particles was achieved by tailoring the Ni loadings in the LDH nanocomposites. Further, the size of the negatively charged Ni hydroxy citrate colloids in the intercalated LDH allows the size of the Ni particles in the supported Ni catalyst to be tuned [64]. However, the resultant mixed oxides were highly stabilized. The reconstruction was prevented due to a strong interaction between the reduced Ni particles and the Mg(Al)O mixed oxides. These Ni supported materials offer promising application in catalysis. The $[Ni(C_6H_4O_7)]^{2-}$-intercalated Mg/Al-LDHs have been prepared by ion-exchange method [65], implying that the subsequent calcination might lead to the formation of well-dispersed nickel ions in a matrix of Mg(Al)O mixed oxide. As stated above, the intercalation and calcination of transition-metal-containing LDHs could be ideal catalyst precursors for supported metal catalysts with small particle size and high dispersion.

3.2.2 *Precursors of Complex Metal Oxide Catalysts*

In the past several years, environmental-friendly complex metal oxide photocatalysts derived from LDHs with long life and excellent catalytic activity have been used heterogeneous catalysts in a variety of reactions. For example, a self-generated template pathway has been used by Zou et al. to prepare complex metal oxide $ZnAl_2O_4$ spinel photocatalysts with mesopore network and high surface areas by Zn/Al-LDH precursor [66]. This synthesis strategy involved calcination of the precursor at 500 °C or above, followed by selective leaching of zinc oxide phase from the resultant calcined products. This led to the formation of single $ZnAl_2O_4$ spinel phase instead of the usually mixed oxides after calcination at 500 °C, whose specific surface area were as high as 253 m^2/g. It was believed that the templating effect of ZnO phase is the essential factor directing the formation of the present high-surface-area spinels with interconnected mesopore network. $ZnAl_2O_4$ spinels displayed higher activity in photo-decomposition of phenol aqueous solution under UV irradiation, compared to $ZnAl_2O_4$ sample prepared by the conventional solid-state method at 1,000 °C. The conversion of phenol reached up to 69% for the $ZnAl_2O_4$ sample calcined at 500 °C, much higher than that for the sample prepared by the solid-state reaction. This high activity originated from high surface area and small pore size of spinels obtained by a precursor route. Moreover, Meng et al. prepared the Zn/Fe-LDHs sulfate with Zn^{II}/Fe^{III} ratios of 2, 3 and 4 [67]. Due to their low thermal stability (the decomposition process is essentially complete at 300 °C), a mixture of ZnO and complex metal oxide $ZnFe_2O_4$ phases could be obtained by calcining the precursors at 500 °C or above. After select leaching of ZnO, as-synthesized pure zinc ferrite with high surface area and pore volume exhibited high catalytic activity for photodegradation of phenol and selectivity to low molecular weigh oxidation products. In the case of the LDH-derived zinc ferrite, competitive adsorption of intermediate products is less significant, this may reflect the higher porosity, which allows easier diffusion of these products away from the initial adsorption site.

Ti-containing inorganic solids have attracted much attention owing to their multi-functionality especially in energy conversion and catalytic reactions. Several groups have reported the synthesis of Ti-containing LDHs [68–72], which make up a new class of Ti-containing inorganic materials with great applications. He et al. reported a Ti-containing nanocomposite from thermal conversion of Ni/Ti-LDH [73]. The detailed structural evolution has been studied for a deep insight of thermal process. During the process, the transformation of the metastable complex metal oxide Ni_2TiO_4 spinel phase to the stable $NiTiO_3$ ilmenite phase was observed. TiO_2 could not be observed any more above 700 °C because of its reaction with NiO to form $NiTiO_3$. The phase transformation at calcination temperature below and at 800 °C belonged to the intraparticle reaction, while a phase separation occurred at 900 °C. The Ti-containing nanocomposites exhibited good photocatalytic activities for the degradation of methylene blue under both UV- and visible-light irradiations. The photoabsorption properties of the nanocomposites can be attributed to the cooperative effect of the mixed wide band gap semiconductor nanoparticles in the UV region, which was attributed to the photoabsorption of $NiTiO_3$ in the visible-light region. The Ti-containing nanocomposite can be expected as a potential photo-activated catalyst in improving sunlight efficiency.

3.3 Catalyst Supports

3.3.1 Supports for Active Inorganic and Complex Anions

During the past decade, the intercalation of catalytically active inorganic and complex anions in interlayer space of LDHs has been proofed to be capable of improving catalytic stability and recyclability compared to their properties in the homogeneous catalyst. Generally, the intercalation in the galleries of LDH layers mainly relied on the electrostatic interactions between the intercalated complexes and the positively charged layers. For example, the use of pillared and intercalated LDHs has been reported in a number of catalytic reactions, including the generation of singlet molecular oxygen from H_2O_2 over MoO_4^{2-}-intercalated Mg/Al-LDHs [74] and N-oxidation of tertiary amines over WO_4^{2-}-intercalated Mg/Al-LDHs [75], heterogeneous *cis*-dihydroxylation over WO_4^{2-}-intercalated Mg/Al-LDHs [76], stereoselective epoxidation of R-(+)-limonene over sulfonato-salen-manganese(III) complex-intercalated Zn/Al-LDHs [77] and so on.

More recently, Sels and coworkers used a heterogeneous MoO_4^{2-}-exchanged Mg/Al-LDH catalyst to produce $^1O_2$ from H_2O_2, and demonstrated the usefulness of the $^1O_2$ in organic transformations [78]. The oxidation kinetics was studied in details and the model was proposed for the heterogeneously catalyzed $^1O_2$ generation and peroxide formation. A key assumption in the model was the compartmentalization of the reaction suspension in terms of a compartment close to the catalyst, i.e., the intralamellar and intragranular zones, and a second compartment formed by the bulk solution. The efficiency of singlet oxygen trapping in the MO_4^{2-}-intercalated Mg/Al-LDHs/H_2O_2 system seemed to depend on the location of the MO_4^{2-} in the LDH granule. In the case, the density and the polarity of the LDH powder and the location of the molybdate within the catalyst may have significant effect on the activity and oxidant efficiency.

Lately, we reported a catalyst derived from intercalated Zn/Al-LDHs, which was used for hydroformylation of higher olefine [79]. Many attempts have also been made to support hydroformylation catalysts but there are problems with catalyst stability and selectivity as well as leaching of the catalytic material. Zhang et al. synthesized the *trans*-RhCl(CO)(TPPTS-Na_3)$_2$ and the Zn/Al-LDHs with nitrate anions (Zn/Al = 2, 3, 4) precursors, respectively. Intercalation of the rhodium complex into LDHs was carried out by the method of ion exchange (Fig. 4).

The thermal stability of *trans*-RhCl(CO)(TPPTS)$_2$/Zn/Al-LDHs increased with decreasing Zn/Al molar ratios. This could be related to the fact that the higher Zn/Al molar ratios, the lower content of intercalated guest. As a result, with Zn/Al molar ratios, the hindrance of interlayer

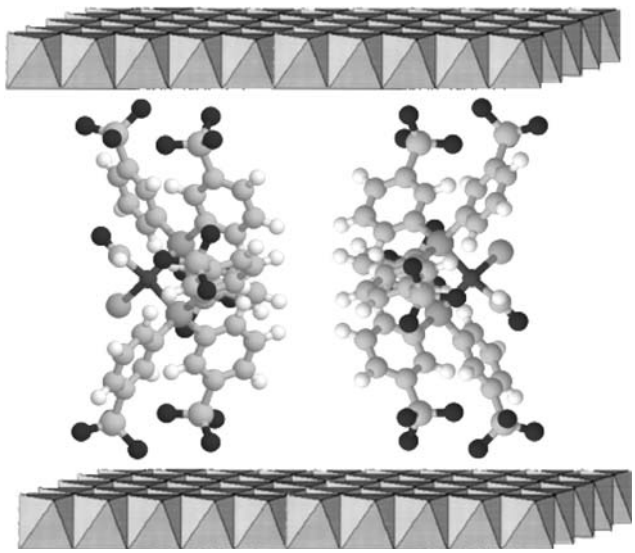

Fig. 4 A schematic representation of the possible arrangement in *trans*-RhCl(CO)(TPPTS)$_2$/Zn/Al-LDH

diffusion for the interlayer guest was decreased and decomposed easier. Compared with that for pure *trans*-RhCl(CO)(TPPTS-Na_3)$_2$, the decomposition of the intercalated anions was postponed and the combustion temperature was increased by ca. 110 °C due to the interlayer confined effect. Therefore, the intercalation of such rhodium complexes into LDHs may have potential applications in the development of novel supported aqueous-phase catalysts for hydroformylation of higher olefins. Wei and coworkers further investigated the catalytic performance of the *trans*-RhCl(CO)(TPPTS)$_2$ and TPPTS ligand cointercalated Zn/Al-LDHs in the hydroformylation of alkenes [80]. The catalyst showed higher activity towards aldehyde formation and better reusability compared with the corresponding water–oil biphasic catalytic system under similar reaction conditions. Strong interactions between the LDH layers and the active rhodium species on intercalation led to the good reusability. In addition, the catalyst prepared by the in situ complexation method exhibited much higher catalytic activity and selectivity towards aldehydes compared with that of an intercalated complex prepared by ion-exchange method. Increasing the Zn/Al molar ratio in the catalyst led to lower activity and higher selectivity to both total aldehyde and *n*-aldehyde, which can be related to the content of Rh and the availability of the free ligands, respectively.

If the interlayer surfaces of LDHs are modified by a covalent linking agent, such as an organosilane, many unprecedented properties as a matrix and affinities for various organic or inorganic guests can be expected. Kim et al. studied interlayer surface modification of LDHs with oxane bonds M–O–Si (M = Zn and Cr) [81], where the condensation of hydroxyl groups of LDHs sheet and ethoxy

groups of (3-ami-nopropyl)triethoxysilane (APS) took place. Since the galleries of these modified LDHs had a hydrophobic field, a variety of functional molecules such as catalysts, enzymes, or chiral molecules with organic characteristics can readily be incorporated into the interlayer of LDHs. Also, the APS-modified LDHs can be applied in heterogeneous catalysis for various organic reactions, e.g., to produce alkylated amines.

3.3.2 Immobilization Supports for Biomolecules

Much attention has been paid to the intercalation of biomolecules into LDHs. Based on the results obtained in our laboratory we have reported the immobilization of enzyme in the interlayer of LDHs and their catalytic efficiency. For example, He et al. studied the immobilization of penicillin G acylase in Mg/Al-LDH pillared by glutamate ions [82]. Wei et al. have achieved the intercalation of L-Aspartic acid (L-Asp) into Mg/Al-LDHs by a coprecipitation method [83, 84]. The investigation of structural model revealed that the guest anions were accommodated in the interlayer region as a monolayer with the two carboxylate groups electrostatically attracted to both upper and lower hydroxide layers, with a hydrogen-bonding network existing between water, the guest anions, and the host layers. The thermolysis of L-Asp LDH involved three steps. The first step was the loss of both adsorbed and interlayer water occurring between room temperature and 150 °C. The second one was the polymerization and deamination of L-Asp ions in the interlayer of LDH and dehydroxylation of the brucite-like layers beginning at 250 °C. The third step in the range of 350–450 °C corresponded to dehydroxylation of the brucite-like layers as well as further decomposition of interlayer materials. They also studied the intercalation of L-Tyrosine (L-Tyr) in Ni/Al-, Mg/Al- and Zn/Al-LDHs [85]. Intercalation of L-Tyr can prevent its racemization under sunlight, heat or UV light. The observed increase in photochemical stability could be due to racemization of the chiral guest being restricted significantly in the galleries of the host layers as a result of the host–guest and guest–guest interactions. Therefore, this layered material may have potential application as a "molecular container" for storing or transporting unstable chiral biomolecules or pharmaceutical agents. They found that the phase transformation of L-Tyr/LDH composites included the destruction of the hydrogen bonding area resulting from the loss of the interlayer water, the decomposition of the intercalated L-Tyr anions and the dehydroxylation of the host layers [86]. More recently, Wei et al. prepared L-Cystine(L-Cys) and L-Cysteine((L-CysH) intercalated Mg/Al-LDHs by the method of coprecipitation and ion-exchange [87]. According to the experimental conditions for L-CysH intercalated Mg/Al-LDHs with the pH at 10.5, the L-CysH anions existed mainly as divalent anion $^{-}OOCCHNH_2CH_2S^{-}$ and they were accommodated vertically in the interlayer region as a monolayer with the two negative groups of individual anions attracted electrostatically to upper and lower hydroxide layers. The L-CysH anions existed mainly as monovalent anion $^{-}OOCCHNH_2CH_2SH$ during the intercalation process under pH at 8.5, so they were accommodated bilayer arrangement with the carboxyl of individual anions attaching alternately to the upper and lower hydroxide layers.

The LDHs may have prospective application as novel reactors for confined chemical reactions, and new opportunities for further research into molecular reactions in the nanoscale of inorganic hybrids and for their applications in catalysis and separation sciences. The oxidation of L-CysH intercalated LDHs by hydrogen peroxide and bromine has been studied [88], respectively. The oxidation of L-CysH intercalated LDHs was carried out by adding H_2O_2 to the aqueous suspension of L-CysH intercalated LDHs. The gallery height of the oxidation product of L-CysH intercalated LDHs was 0.72 nm, smaller than the calculated length of L-Cys molecule (0.97 nm). The results suggested that the oxidation product L-Cys might be accommodated obliquely to the host layer, in which the oblique angle was $\sim 48°$ between the host layer and the L-Cys molecular chains. The oxidation reaction of cysteine was rather different within the LDHs interlayers from that of its free form in solution. The oxidation product of cysteine was only cysteic acid in the confined region of interlayers, independent of the quantity of Br_2. This was because that the diffusion of Br_2 in the LDH interlayers was the rate-determining step for the interlayer oxidation reaction of L-CysH. At the first stage, Br_2 molecules diffused into the interlayer edges of LDHs and oxidized cysteine to cystine. Then, further oxidation of cystine to cysteic acid occurred owing to quite faster rate of reaction, compared with the diffusion rate of Br_2. As a result, only cysteic acid was obtained regardless of the quantity of oxidant Br_2.

He et al. presented a detailed investigation of the preparation and characterization of L-proline intercalated LDHs (L-Pro LDHs) by the "memory effect," along with its application in a typical aldol reaction between acetone and benzaldehyde [89] (See Fig. 5). The immobilization of L-proline on LDHs significantly inhibits the racemization of L-proline anions, effectively enhancing the thermal and optical stability.

Asymmetric aldol reaction of benzaldehyde and acetone was carried out using L-Pro LDHs as catalyst, resulting in a good yield and a high enantiomeric excess (ee) (See Table 2). Thus L-Pro LDHs as a heterogeneous asymmetric catalyst in aldol reactions exhibits high enantioselectivity even when exposed to rigorous conditions. The stabilization of enantiomeric selectivity on thermal treatment gave

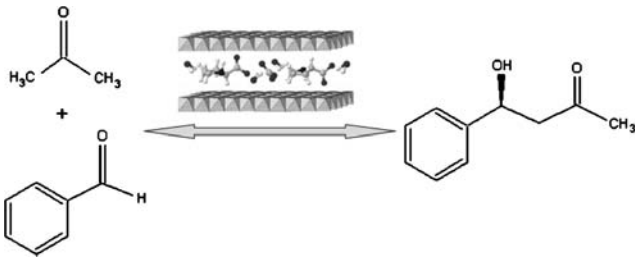

Fig. 5 The schematic representation of aldol reaction between benzaldehyde and acetone catalyzed by L-proline intercalated Mg/Al-LDHs

Table 2 The yield and ee for aldol reaction catalyzed by L-Pro MgAl-LDHs (Mg/Al of 3:1, intercalated yield of 59%) in acetone

Reaction temperature/K	Yield/%	ee/%
293	80	93
313	88	94
Boiling point	89	94

L-Pro LDHs advantages in storage, delivery, and application processes.

In, addition, the calcined LDH has been used as the novel biomolecular vessel for the immobilization, storage as well as release of bromelain [90]. The optimum initial amount of bromelain was 20 mL of 4 mg/mL for 1 g calcined LDH and the immobilized enzyme activity express was 33.4% at pH 6.5, and the Langmuir model can be used to describe the adsorption of bromelain by calcined LDH. It was found that the immobilized bromelain is more stable than that of the free one in the higher temperature rang, and the release behavior of bromelain was based on the "memory effect" of LDHs.

3.3.3 Supports for Noble Metals

LDHs have received much attention in view of their potential usefulness as catalyst support. In such cases, metal–support interaction and metal–support cooperation (metal–base bifunctional catalysis) were put forward to interpret the reactivity of these catalyst materials. For example, the highest selectivity was achieved in the hydrogenation of phenol to cyclohexanone on Pd/Mg(Al)O [91], and in the aromatization of *n*-hexane on Pt, Pd/Mg(Al)O [92], as well in the "one-pot" synthesis of methyl isobutyl ketone from acetone on Pd/Mg(Al)O [93, 94].

Nanopalladium (0) supported Mg/Al-LDHs was investigated for a variety of liquid-phase heterogeneous catalytic reactions by Choudary and coworkers in details [95]. It was found that the nanopalladium immobilized LDH (LDH-Pd^0) catalyzed Heck olefination of electron-poor and electron-rich chloroarenes in nonaqueous ionic liquids and microwave conditions with excellent yields and high turnover frequency. The Mg/Al-LDH supports with the basicity facilitated the Heck olefination reaction, and therefore exhibited the higher reactivity over other heterogeneous catalysts involving resin-Pd^0, Pd/C, Pd/Al_2O_3 and Pd/SiO_2. LDH-Pd^0 catalyst used in Suzuki-, Sonogashira-, and Stille-type coupling reactions of chloraorenes was superior to those of the best homogeneous ligand-free $PdCl_2$ catalysts and as well heterogeneous and nanopalladium supported catalysts. According to Choudary and coworkers, LDH-supported nanoplatinum(0) and nanopalladium(0) catalysts were prepared by a simple ion exchange technique and subsequent reduction with hydrazine hydrate. The catalysts have been used for the allylation of aldehydes to give moderate to good yields of homoallylic alcohols [96]. The acid–base properties and the nature of Pd phase in view of Pd/Mg(Al)O catalysts were further revealed to be relevant with the metal–support interactions [97]. Palladium catalysts with Pd loading of 0.05–1.5 wt% were prepared by impregnation technique with either Pd acetylacetonate or Pd chloride onto Mg(Al)O mixed oxides obtained from thermal decomposition of LDH materials. Pd catalysts obtained by the acetylacetonate precursor showed strongly basic oxygen ions, similar to those of MgO, along with Al^{3+} Lewis acid sites. A peculiar characteristic of these catalysts was the presence of Pd sites, either isolated or in very small clusters, strongly interacting with the basic oxygen anions of the support, resulting in typical metal–support interaction. These sites were responsible for a characteristic of carbonyl species showing unusual active features. The impregnation of $PdCl_2$ had an impact on both acid–base properties and nature of Pd phases, which depended on the ability of the oxide support in retaining chlorine. CO adsorption revealed the presence of Pd oxy-chloride phase, while isolated Pd sites strongly interacting with the basic support were partially or totally depleted, which depended on the chlorine concentration. Moreover, Pd particles obtained by $PdCl_2$ precursor, displayed larger particle sizes and broader particle size distributions compared to those obtained from the acetylacetonate precursor. Interestingly, Ebitani et al. reported that robust heterotrimetallic $Ru^{IV}Mn^{IV}Mn^{IV}$ species coordinated to LDH surface showed highly efficient heterogeneous catalytic ability for liquid-phase oxidation of alcohols by molecular oxygen at atmospheric pressure [32].

3.3.4 Magnetic Supports

Complex metal oxides derived from LDHs are suitable precursors for magnetic catalyst supports. The $NiFe_2O_4$ spinel ferrites were obtained from $Ni^{2+}/Fe^{2+}/Fe^{3+}$-LDHs precursors by Li et al. [98]. The magnetic property

possessed higher value of specific saturation magnetization and lower values of coercivity than $MgFe_2O_4$ and $CoFe_2O_4$ materials. Therefore, $NiFe_2O_4$, the best combination of soft magnetic property, were coated with silica and then used as magnetic cores for the preparation of porous micro-spherical alumina particles by the oil column method. The resulting $NiFe_2O_4$–SiO_2–Al_2O_3 composite material existed as well-formed spherical particles with smooth surfaces, excellent specific surface area (191 $m^2\ g^{-1}$) and the specific saturation magnetization (7.21 emu g^{-1}), thus the composite property was suitable for practical applications as a catalyst or catalyst support. Recently, Lu et al. also reported a nanoscale magnetic photocatalyst (TiO_2/SiO_2/$CoFe_2O_4$) for degradation of methyl orange dye [99]. The $CoFe_2O_4$ nanoparticles with high magnetization as magnetic core were prepared from Co^{2+}/Fe^{2+}/Fe^{3+}-SO_4^{2-}-LDHs precursor.

3.4 Microreactors

In recent years, considerable interest has been devoted to nanocomposites prepared from the assembly of an organic polymer and an inorganic layered material. Duan et al. had prepared styrene sulfonate intercalated Mg/Al-LDHs (SS-LDHs) by a coprecipitation method. The in situ polymerization of the monomers in the interlayer space of LDH was studied [100]. When the obtained SS-LDHs was heated at 150 °C to afford the polymerization of the intercalated monomer, the monomer polymerized completely and the polymer intercalated PSS-LDHs was obtained. The polymerization of metanilic (m-$NH_2C_6H_4SO_3^-$) within the interlayer of Ni/Al-LDHs by using nitrate and ammonium persulfate as oxidizing agents was investigated, respectively [101, 102]. The advantages of preparing polyaniline (PANI) Ni/Al-LDHs nanocomposites by using pre-intercalated nitrate as an oxidizing agent were that the restricted interlayer region of the LDHs makes it easier to obtain nanosized oligomers with uniform size and that the pre-intercalated NO_3^- acting as an oxidizing agent can prevent the influence of mass transfer and diffusion on the polymerization reaction of the interlayer monomer. They found that through in situ techniques the polymerization of the interlayer monomer under a nitrogen atmosphere heating at 300 °C, and the coupling between monomers most likely occurs by the (α,β) and (N,N) linkages. The oxidative polymerization of the metanilic anion between the sheets of Ni/Al-LDH can be interpreted as follows: the m-$NH_2C_6H_4SO_3$ anions intercalated in Ni/Al-LDH are in an interpenetrating arrangement. Water molecules and co-existing nitrate anions occupy the interlayer interstices. Following the addition of an oxidizing agent, $S_2O_8^{2-}$ intercalated into the host layer by ion-exchange with NO_3^- and initiated the oxidative polymerization of the interlayer monomer.

4 Conclusion

LDHs represent one of the most technologically promising materials as a consequence of their low cost, relative ease of preparation, and the large number of composition/preparation variables that may be adopted. At present, even though a great deal of applications of LDHs materials in catalysis, covering a wide range of areas, have made substantial progress, especially over the past decade. However, synthesis of high-quality LDHs and derived materials in a controlled manner, and detailed understanding of the catalytic mechanisms are still challenges to be faced in the future.

Acknowledgments The authors gratefully acknowledge the financial support from the National Natural Science Foundation of China and 973 Program (2009CB939802).

References

1. Cavani F, Trifiro F, Vaccari A (1991) Catal Today 11:173
2. Khan AI, O'Hare D (2002) J Mater Chem 12:3191
3. He J, Wei M, Li B, Kang Y, Evans DG, Duan X (2006) Struct Bond 119:89
4. Evans DG, Duan X (2006) Chem Commun 485
5. Williams GR, O'Hare D (2006) J Mater Chem 16:3065
6. Sileo EE, Jobbágy M, Paiva-Santos CO, Regazzoni AE (2005) J Phys Chem B 109:10137
7. Rao MM, Reddy BR, Jayalakshmi M, Jaya VS, Sridhar B (2005) Mater Res Bull 40:347
8. Iyi N, Matsumoto T, Kanoko Y, Kitamura K (2004) Chem Lett 33:1122
9. Han YF, Liu ZH, Yang ZP, Wang ZL, Tang XH, Wang T, Fan LH, Ooi K (2008) Chem Mater 20:360
10. Lei XD, Yang L, Zhang FZ, Duan X (2006) Chem Eng Sci 61:2730
11. Zhao Y, Li F, Zhang R, Evans DG, Duan X (2002) Chem Mater 14:4286
12. Xu ZP, Stevenson GS, Lu CQ, Lu GQ, Bartlett PF, Gray PP (2006) J Am Chem Soc 128:36
13. Hu G, O'Hare D (2005) J Am Chem Soc 127:17808
14. Hu G, Wang N, O'Hare D, Davis J (2006) Chem Commun 287
15. Li L, Ma RZ, Iyi N, Ebina Y, Takada K, Sasaki T (2006) Chem Commun 3125
16. Ge′raud E, Pre′vot V, Ghanbaja J, Leroux F (2006) Chem Mater 18:238
17. Géraud E, Rafqah S, Sarakha M, Forano C, Prevot V, Leroux F (2008) Chem Mater 20:1116
18. Gardner E, Huntoon KM, Pinnavaia TJ (2001) Adv Mater 13:1263
19. Lee JH, Rhee SW, Jung DY (2003) Chem Commun 2740
20. Lee JH, Rhee SW, Jung DY (2004) Chem Mater 16:3774
21. Lee JH, Rhee SW, Jung DY (2007) J Am Chem Soc 129:3522
22. Lei XD, Yang L, Zhang FZ, Evans DG, Duan X (2005) Chem Lett 34:1610
23. Lv Z, Zhang FZ, Lei XD, Yang L, Evans DG, Duan X (2007) Chem Eng Sci 62:6069
24. Chen HY, Zhang FZ, Fu SS, Duan X (2006) Adv Mater 18:3089
25. Wang LY, Li C, Liu M, Evans DG, Duan X (2007) Chem Commun 123
26. Cosimo DJ, Diez VK, Xu M, Iglesia E, Apesteguia CR (1998) J Catal 178:499

27. Abelló S, Medina F, Tichit D, Péréz-Ramírez J, Rodríguez X, Sueiras JE, Salagre P, Cesteros Y (2005) Appl Catal A 281:191
28. Nishimura T, Kakiuchi N, Inoue M, Uemura S (2000) Chem Commun 1245
29. Constantino VRL, Pinnavaia TJ (1995) Inorg Chem 34:883
30. Abello′ S, Medina F, Tichit D, Pe′rez-Ramı′rez J, Groen JC, Sueiras JE, Salagre P, Cesteros Y (2005) J Chem Eur 11:728
31. Roeffaers MJ, Sels BF, Uji-I H, De Schryver FC, Jacobs PA, De-Vos DE, Hofkens J (2006) Nature 439:572
32. Ebitani K, Motokura K, Mizugaki T, Kaneda K (2005) Angew Chem Int Ed 44:3423
33. Lei XD, Zhang FZ, Yang L, Guo XX, Tian YY, Fu SS, Li F, Evans DG, Duan X (2007) AIChE J 53:932
34. Abello′ S, Medina F, Tichit D, Pe′rez-Ramı′rez J, Cesteros Y, Salagre P, Sueiras JE (2005) Chem Commun 1453
35. Roelofs JCAA, Lensveld DJ, Van Dillen AJ, De Jong KP (2001) J Catal 203:184
36. Lv Z, Zhang FZ, Lei XD, Yang L, Xu SL, Duan X (2008) Chem Eng Sci 63:4055
37. Zhang H, Qi R, Evans DG, Duan X (2004) J Solid State Chem 177:772
38. Winter F, Van Dillen AJ, De Jong KP (2005) Chem Commun 3977
39. Li F, Jiang XR, Evans DG, Duan X (2005) J Porous Mater 12:55
40. Wang YC, Zhang FZ, Xu SL, Yang L, Li DQ, Evans DG, Duan X (2008) Chem Eng Sci 63:4306
41. Choudary BM, Kantam ML, Kavita B, Reddy CV, Figueras F (2000) Tetrahedron 56:9369
42. Choudary BM, Kantam ML, Neeraja V, Rao KK, Figueras F, Delmotte L (2001) Green Chem 3:257
43. Choudary BM, Kantam ML, Reddy CV, Bharathi B, Figueras F (2003) J Catal 218:191
44. Kantam ML, Ravindra A, Reddy CV, Sreedhar B, Choudary BM (2006) Adv Synth Catal 4/5:569
45. Velu S, Suzuki K, Osaki T (2000) Catal Lett 69:43
46. Zhang LH, Li F, Evans DG, Duan X (2004) Mater Chem Phys 87:402
47. Li F, Zhang LH, Evans DG, Duan X (2004) Colloids Surfaces A 244:169
48. Matsumoto S (1996) Catal Today 29:43
49. Shinjoh H, Takahashi N, Yokota K, Sugiura M (1998) Appl Catal B 15:189
50. Prinetto F, Ghiotti G, Nova I, Lietti L, Tronconi E, Forzatti P (2001) J Phys Chem B 105:12732
51. Olsson L, Persson H, Fridell E, Skoglundh M, Andersson B (2001) J Phys Chem B 105:6895
52. Centi G, Fornasari G, Gobbi C, Livi M, Trifirò F, Vaccari A (2002) Catal Today 73:287
53. Fornasari G, Glöckler R, Livi M, Vaccari A (2005) Appl Clay Sci 29:258
54. Palomares AE, Lopez-Nieto JM, Lazaro FJ, Lopez A, Corma A (1999) Appl Catal B 20:257
55. Yu JJ, Wang XP, Tao YX, Hao ZP, Xu ZP (2007) Ind Eng Chem Res 46:5794
56. Yu JJ, Wang XP, Li LD, Hao ZP, Xu ZP, Lu GQ (2007) Adv Funct Mater 17:3598
57. Li F, Tan Q, Evans DG, Duan X (2005) Catal Lett 99:151
58. Hima HI, Xiang X, Zhang L, Li F (2008) J Mater Chem 18:1245
59. Xiang X, Hima HI, Wang H, Li F (2008) Chem Mater 20:1173
60. Tichit D, Coq B (2003) Cattech 6:206
61. Shishido T, Sukenobu M, Morioka H, Furukawa R, Shirahase H, Takehira K (2001) Catal Lett 1:21
62. Olafsen A, Slagtern Å, Dahl IM, Olsbye U, Schuurman Y, Mirodatos C (2005) J Catal 229:163
63. Gérardin C, Kostadinova D, Sanson N, Coq B, Tichit D (2005) Chem Mater 17:6473
64. Gérardin C, Kostadinova D, Coq B, Tichit D (2008) Chem Mater 20:2086
65. Wang LY, Wu GQ, Evans DG (2007) Mater Chem Phys 104:133
66. Zou L, Li F, Xiang X, Evans DG, Duan X (2006) Chem Mater 18:5852
67. Meng WQ, Li F, Evans DG, Duan X (2004) J Porous Mater 11:97
68. Saber O, Hatano B, Tagaya H (2005) J Inclusion Phenom Macrocyclic Chem 51:17
69. Saber O, Tagaya H (2003) J Inclusion Phenom Macrocyclic Chem 45:109
70. Saber O, Hatano B, Tagaya H (2005) Mater Sci Eng C 25:462
71. Das N, Samal A (2004) Micropor Mesopor Mat 72:219
72. Shu X, Zhang WH, He J, Gao FX, Zhu YX (2006) Solid State Sci 8:634
73. Shu X, He J, Chen D, Wang YX (2008) J Phys Chem C 112:4151
74. Laar FV, Vos DD, Vanoppen D, Sels B, Jacobs PA, Del Guerzo A, Pierard F, Kirsch-De Mesmaeker A (1998) Chem Commun 267
75. Choudary BM, Bharathi B, Venkat Reddy Ch, Lakshmi Kantam M, Raghavan KV (2001) Chem Commun 1736
76. Severeyns A, De Vos DE, Jacobs PA (2002) Green Chem 4:380
77. Bhattacharjee S, Anderson JA (2004) Chem Commun 554
78. Sels BF, De Vos DE, Jacobs PA (2007) J Am Chem Soc 129:6916
79. Zhang X, Wei M, Pu M, Li XJ, Chen H, Evans DG, Duan X (2005) J Solid State Chem 178:2701
80. Wei M, Zhang X, Evans DG, Duan X, Li XJ, Chen H (2007) AIChE J 53:2911
81. Park AY, Kwon H, Woo AJ, Kim SJ (2005) Adv Mater 17:106
82. Ren LL, He J, Zhang SC, Evans DG, Duan X (2002) J Mol Catal B 18:11
83. Yuan Q, Wei M, Evans DG, Duan X (2004) J Phys Chem B 108:12381
84. Yuan Q, Wei M, Wang ZQ, Wang G, Duan X (2004) Clay Clay Miner 52:40
85. Wei M, Yuan Q, Evans DG, Wang ZQ, Duan X (2005) J Mater Chem 15:1197
86. Wei M, Xu XY, He J, Yuan Q, Rao GY, Evans DG, Pu M, Yang L (2006) J Phys Chem Solids 67:1469
87. Wei M, Guo J, Shi ZY, Yuan Q, Pu M, Rao GY, Duan X (2007) J Mater Sci 42:2684
88. Wei M, Shi ZY, Evans DG, Duan X (2006) J Mater Chem 16:2102
89. An Z, Zhang WH, Shi HM, He J (2006) J Catal 241:319
90. Shi WY, Wei M, Jin L, Li CJ (2007) J Mol Catal B 47:58
91. Chen YZ, Liaw CW, Lee LI (1999) Appl Catal A 177:1
92. Davis J, Derouane EG (1991) Nature 349:313
93. Chen YZ, Hwang CM, Liaw CW (1998) Appl Catal A 169:207
94. Das N, Tichit D, Graffin P, Coq B (2001) Catal Today 71:181
95. Choudary BM, Madhi S, Chowdari NS, Kantam ML, Sreedhar B (2002) J Am Chem Soc 124:14127
96. Choudary BM, Roy M, Roy S, Kantam ML, Jyothi K, Sreedhar B (2005) Adv Synth Catal 15:2009
97. Prinetto F, Manzoli M, Ghiotti G, Ortiz MJM, Tichit D, Coq B (2004) J Catal 222:238
98. Feng JT, Lin YJ, Li F, Evans DG, Li DQ (2007) Appl Catal A 329:112
99. Lu ZL, Zhang H, Duan X (2006) Adv Mater Res 11/12:611
100. Si LC, Wang G, Cai FL, Wang ZQ, Duan X (2004) Chin Sci Bull 23:2459
101. Wei M, Tian XF, He J, Pu M, Rao GY, Yang HL, Yang L, Liu T, Evans DG, Duan X (2006) Eur J Inorg Chem 3442
102. Tian XF, Wei M, Evans DG, Rao GY (2006) Clay Clay Miner 4:418